Design and use of an Elsässer probe for analysis of Alfvén wave fields according to wave direction

D. J. Drake,[1] C. A. Kletzing,[1] F. Skiff,[1] G. G. Howes,[1] and S. Vincena[2]
[1]*Department of Physics and Astronomy, University of Iowa, Iowa City, Iowa 52242, USA*
[2]*Department of Physics, University of California at Los Angeles, Los Angeles, California 90095, USA*

(Received 2 August 2011; accepted 20 September 2011; published online 17 October 2011)

We have designed an electric and magnetic field probe which simultaneously measure both quantities in the directions perpendicular to the background magnetic field for application to Alfvén wave experiments in the Large Plasma Device at UCLA. This new probe allows for the projection of measured wave fields onto generalized Elsässer variables. Experiments were conducted in a singly ionized He plasma at 1850 G in which propagation of Alfvén waves was observed using this new probe. We demonstrate that a clear separation of transmitted and reflected signals and determination of Poynting flux and Elsässer variables can be achieved. © *2011 American Institute of Physics*. [doi:10.1063/1.3649950]

I. INTRODUCTION

First predicted by H. Alfvén in 1942,[1] Alfvén waves have become one of the most studied plasma waves because of their numerous applications to space physics[2–5] and magnetically confined plasmas.[6,7] To measure these waves, both magnetic and electric field probes have been employed. The most common type of magnetic field probe is a Mirnov coil,[8] also known as a magnetic loop probe, or "b-dot" probe. When a time varying magnetic field passes through the coil, a voltage is induced in the wire. By using Faraday's law, the magnetic field can be determined from the voltage by time integration of the measured signal. Mirnov coils have long been used to measure magnetic fields on the outside edge of tokamaks.[9,10] These types of probes have also been applied to the measurement of waves in linear plasma columns. Thuecks *et al.*[11] used a probe consisting of three orthogonally placed Mirnov coils (triple axis probe) to measure the vector magnetic field of an Alfvén wave produced by an arbitrary spatial waveform antenna.[12] Further experiments by this group used this tool to measure the damping rates of the waves under different plasma conditions.

The double probe is the most frequently used technique for measurement of an electric field in plasmas. The basic idea is that the electric field can be determined by measuring the voltage difference at two radially separated probe points divided by their distance apart.[13] This type of probe was successfully used on a wide range of space missions, including the ISEE-1, DE-2, Freja, and Cluster satellites, to measure electric fields in ionospheric[14] and magnetospheric[15,16] plasmas. One of the main problems with this tool for laboratory plasmas, as with other electric probes, is that they have limited bandwidth. Most electric probes are connected to amplifiers outside the plasma by long pieces of coaxial cable, which have an internal capacitance that limits the bandwidth of the probe. One way to solve this problem is by capacitance neutralization.[17] In this technique a double shielded cable is employed with a unity-gain amplifier connected between the center wire and the inner shield. This will effectively reduce the capacitance in the cable to nearly zero and, subsequently, the losses at high frequencies will be reduced. However, instability issues can arise with this method which can further limit the bandwidth. Another problem with the double probe technique is that electrostatic pick-up from drift waves,[18] typically very strong near the plasma edge, can make measurements of the electric field very noisy in laboratory plasmas, which can subsequently limit the sensitivity of the probe. The simplest approach to suppressing low frequency drift waves is to add a high pass filter circuit. This method has long been used with laboratory plasma probes[19,20] and satellites/orbiters.[21]

We present a new type of diagnostic tool, that we call the Elsässer probe, which can be used to measure simultaneously the electric and magnetic fields of a plasma wave. In our implementation, we measure wave fields in the plane perpendicular to a fixed magnetic field in the plasma. In Sec. II, we discuss the theory of the Elsässer probe and the relationship between the Elsässer variables and the measured quantities. In Sec. III, we describe the construction and calibration of the probe and also discuss how to offset effectively the need for the capacitance neutralization technique. In Sec. IV, we present the experimental conditions used to test this new type of probe. In addition, we show data from the probe and discuss the results in terms of the theory.

II. ELSÄSSER PROBE THEORY

For an ideal, incompressible MHD plasma, the equations of evolution are given by

$$\frac{\partial \mathbf{v}}{\partial t} + \mathbf{v}\cdot\nabla\mathbf{v} = -\frac{\nabla p}{\rho_0} + \frac{\mathbf{B}\cdot\nabla\mathbf{B}}{\mu_0\rho_0}, \tag{1}$$

$$\frac{\partial \mathbf{B}}{\partial t} + \mathbf{v}\cdot\nabla\mathbf{B} = \mathbf{B}\cdot\nabla\mathbf{v}, \tag{2}$$

$$\nabla\cdot\mathbf{v} = 0, \quad \nabla\cdot\mathbf{B} = 0, \tag{3}$$

where $\mathbf{v}$ is the fluid velocity, $\mathbf{B}$ is the magnetic field, p is the thermal pressure, μ_0 is the permeability of free space, and ρ_0

is the density. Note that the density ρ_0 is a constant in incompressible MHD. Elsässer first recognized that, when the magnetic field is expressed in velocity units as $\mathbf{B}/\sqrt{\mu_0\rho_0}$, the equations have a symmetric form.[22] By adding and subtracting Eqs. (1) and (2), the equations for incompressible MHD can be expressed in the symmetric form

$$\frac{\partial \mathbf{z}^{\pm}}{\partial t} \mp \mathbf{V}_A \cdot \nabla \mathbf{z}^{\pm} + \mathbf{z}^{\mp} \cdot \nabla \mathbf{z}^{\pm} = -\frac{\nabla p}{\rho_0}, \tag{4}$$

where the magnetic field has been decomposed into its equilibrium and fluctuating parts $\mathbf{B} = \mathbf{B}_0 + \delta\mathbf{B}$, the Alfvén velocity due to the equilibrium magnetic field $\mathbf{B}_0$ is given by $\mathbf{V}_A = \mathbf{B}_0/\sqrt{\mu_0\rho_0}$, and $\mathbf{z}^{\pm} = \mathbf{v} \pm \delta\mathbf{B}/\sqrt{\mu_0\rho_0}$ are the Elsässer variables. The Elsässer variables $\mathbf{z}^{+}$ represent a wave traveling down the mean magnetic field and $\mathbf{z}^{-}$ is a wave traveling up the magnetic field. The second term on the left-hand side of Eq. (4) represents the linear propagation of the Elsässer variables along the mean magnetic field at the Alfvén speed, while the third term represents the nonlinear interaction between parallel and anti-parallel propagating waves. The pressure gradient ensures impressibility of the fluctuations.

The Elsässer variables can be used to separate Alfvén waves traveling up the magnetic field from those traveling down the field by adding and subtracting the velocity and magnetic field fluctuations. This property can be exploited to design an Elsässer probe that can distinguish counter-propagating Alfvén wave signals measured in the laboratory. Although laboratory plasmas are not generally well described as incompressible MHD plasmas, this property of Alfvén waves continues to hold, in a general sense, even when a more detailed plasma description is used, such as cold plasma theory or kinetic theory. In these cases, one must use generalized Elsässer variables to separate the signals from counter-propagating Alfvén waves, as detailed below for the case of cold plasma theory.

Another issue is that direct measurement of the wave velocity perturbation $\mathbf{v}$ in the laboratory is difficult. However, in a magnetized plasma, this fluid wave velocity is simply related to the electric field perturbation. To first order, the linear fluid velocity perturbation is given by the $\mathbf{E} \times \mathbf{B}$ drift in the mean magnetic field, so we may replace the fluid velocity by $\mathbf{v} = \mathbf{E} \times \mathbf{B}_0/\mathbf{B}_0^2$. The generalized Elsässer variables can then be given by

$$\mathbf{z}^{\pm} = C_{cf}\frac{\mathbf{E} \times \mathbf{B}_0}{\mathbf{B}_0^2} \pm \frac{\delta\mathbf{B}}{\sqrt{\mu_0\rho}}, \tag{5}$$

where $\mathbf{E} \times \delta\mathbf{B}$ is the Poynting flux and C_{cf} is a correction factor (which may depend on plasma parameters) to account for deviations arising in the Alfvén wave properties when a more complete plasma description than incompressible MHD is chosen. Below we describe in detail the calculation of this correction factor using cold plasma theory.[23]

To find a relationship between the electric and magnetic field fluctuations for a cold plasma Alfvén wave, we first specify, without loss of generality, a magnetized plasma with equilibrium magnetic field $\mathbf{B}_0 = B_0\hat{z}$ and a linear perturbation with a wave vector $\mathbf{k} = k_x\hat{x} + k_z\hat{z}$. We want to consider the cold plasma limit of the low-frequency Alfvén wave, so we specify a frequency ω that satisfies the limits $kv_{ts} \ll \omega < \Omega_i \ll \omega_{pi}$, where $v_{ts} = \sqrt{2k_BT_s/m_s}$ is the thermal velocity for either species s, Ω_i is the ion cyclotron frequency, and ω_{pi} is the ion plasma frequency. For wave vectors relevant to the Large Plasma Device (LaPD) at UCLA with $k_{\|} \ll k_{\perp}$, the Alfvén wave mode has $\delta B_y \neq 0$ and $\delta B_x = \delta B_z = 0$. After Fourier transforming the Ampére-Maxwell law in both space and time, it is clear that the Alfvén wave mode will have associated electric field components $E_x \neq 0$, $E_z \neq 0$, and $E_y = 0$.

For the chosen cold plasma Alfvén wave limit, the plasma conductivity expresses the x and z components of the current in terms of the x and z components of the electric field,

$$J_z = -i\varepsilon_0\frac{\omega_{pe}^2}{\omega}E_z, \tag{6}$$

$$J_x = -i\varepsilon_0\omega_{pi}^2\frac{E_x}{\omega^2 - \Omega^2}, \tag{7}$$

where ε_0 is the permittivity of free space. Substituting these expressions for the current into the Ampére-Maxwell law, and using Faraday's law to express the magnetic field in terms of the electric field, we obtain a matrix expression with a solvability condition that yields the dispersion relation for cold plasma Alfvén waves,

$$\omega^2 = k_z^2V_A^2\left(\frac{1 - \omega^2/\Omega_i^2}{1 + k_x^2\delta_e^2}\right), \tag{8}$$

where $\delta_e = c/\omega_{pe}$ is the electron skin depth.[24] In the parenthesis, the numerator contains corrections for the limit of finite wave frequency (compared to the ion cyclotron frequency), and the denominator contains the correction for electron inertia at small perpendicular scales.

Substituting Eq. (8) into Eq. (6), we obtain a final expression for E_x (normalized by V_AB_0) in terms of $\delta B_y/B_0$,

$$\frac{E_x}{V_AB_0} = \mp\frac{\delta B_y}{B_0}\sqrt{\left(1 + k_x^2\delta_e^2\right)\left(1 - \frac{\omega^2}{\Omega_i^2}\right)}. \tag{9}$$

For the specified wave vector, the normalized generalized Elsässer variables for the cold plasma Alfvén mode are given by

$$\frac{z^{\pm}}{V_A} = C_{cf}\frac{E_x}{V_AB_0} \pm \frac{\delta B_y}{B_0}. \tag{10}$$

So the correction factor for this system is given by

$$\frac{1}{C_{cf}} = \pm\sqrt{\left(1 + k_x^2\delta_e^2\right)\left(1 - \frac{\omega^2}{\Omega^2}\right)}. \tag{11}$$

Therefore, by adding and subtracting the perpendicular electric and magnetic field measurements with this correction factor, we may distinguish an Alfvén wave traveling up the field (z^-) from one traveling down the field (z^+).

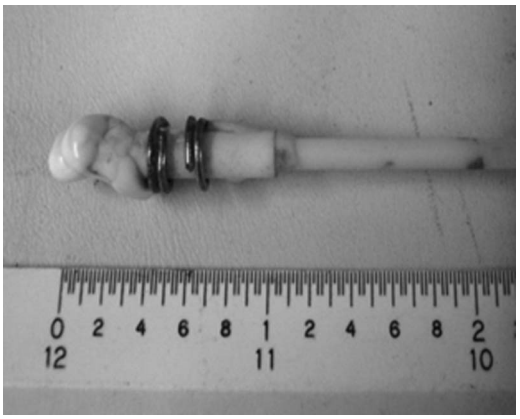

FIG. 1. Picture of the Elsässer probe. The thin insulation of the B-dot (Mirnov) coil magnet wires (at the tip of the probe) are here shown protected from the plasma by a coating of epoxy.

III. DESIGN AND CALIBRATION OF THE ELSÄSSER PROBE

The prototype Elsässer probe was designed to allow for simultaneous measurements of B_x, B_y, and E_x in a plasma, that is, the two components of **B** perpendicular to B_0 and one component of $E_\perp$. To measure the magnetic field components, we constructed two B-dot coils with forty 1.6 mm diameter loops of magnetic wire and oriented them such that one is in the $\hat{x}$ plane and one is in the $\hat{y}$ plane. For the electric field measurements, we have assembled a double probe constructed out of two circular pieces of tantalum wire, allowing for measurement of E_x. Tantalum was chosen since it has a very high melting point. As shown in Fig. 1, the length of the probe from the end of Mirnov coil to the edge of the second E-field wire is 1.9 cm (∼0.75 in.).

A. Design considerations

As discussed above, the main issue with magnetic and electric probes is that they have limited bandwidth due to the internal capacitance of the coaxial cable. To alleviate the need for long pieces of coaxial, we have included an integrated amplifier circuit located 15 cm from the probe end within the vacuum chamber for all three measured components, B_x, B_y, and E_x. Since this distance is short, relative to the lengths of the coaxial cables normally used, the total capacitance in this cable is small, approximately 15 pF. However, this strategy does have one problem associated with it: heating of the electronics. The amplifier circuit is placed in an aluminum box inside of the plasma chamber, which is under vacuum. The combination of the heating from the plasma and the power dissipated by the electronics in the box can cause the circuit to overheat and the amplifiers to go into oscillation or to damage permanently the amplifiers by taking them outside of their specified temperature range. To solve this problem we include a conductive cooling adapter at the end of the aluminum box furthest from the probe tip. A copper block, with a U-shaped cavity drilled through it, is placed at the end of the aluminum box. Two pieces of copper tubing are soldered into each side of the U-shaped cavity. Compressed air, at room temperature,

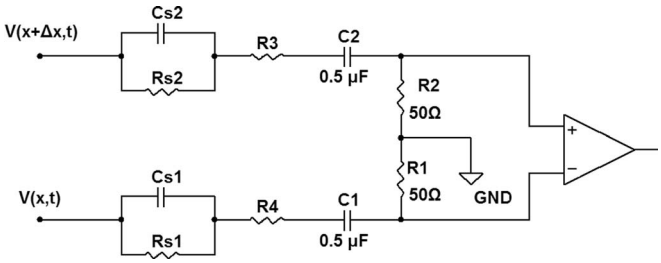

FIG. 2. Circuit diagram for front end of the electric field probe.

is circulated through the tubing allowing for conductive cooling of the box.

Another issue is the effect of the probe sheath on the frequency response. Series capacitors are used on the input to provide protection for the amplifiers from the high dc voltage possible in the cathode discharge and the large amplitude low frequency drift waves. The front end of the E-field probe circuit is shown in Fig. 2. The voltage on the two loops, located at x and $x + \Delta x$, and the sheath capacitance and resistance are shown on the left-hand side of the circuit diagram. Based on the plasma parameters for our experiment (see Sec. IV) and since $\omega_{pi} \gg \omega$, the sheath capacitance is negligible. The sheath impedance for this circuit can be estimated from the derivative of the I-V curve,[25]

$$R_{sh} \approx \frac{\lambda_D}{A\varepsilon_0\omega_{pi}}, \tag{12}$$

where A is the cross-sectional area of the probe and λ_D is the Debye length. In the prototype probe, described here, R3 and R4 were set to 50 Ω. Using Eq. (12), we see that the sheath impedance is close to 550 Ω which is 11 times higher than the circuit input impedance. If R3 and R4 have values lower than the sheath impedance, the RC roll off for this circuit will be dominated by the sheath. Thus, in subsequent versions of the probe we set the value of these two resistors to 10 kΩ, which

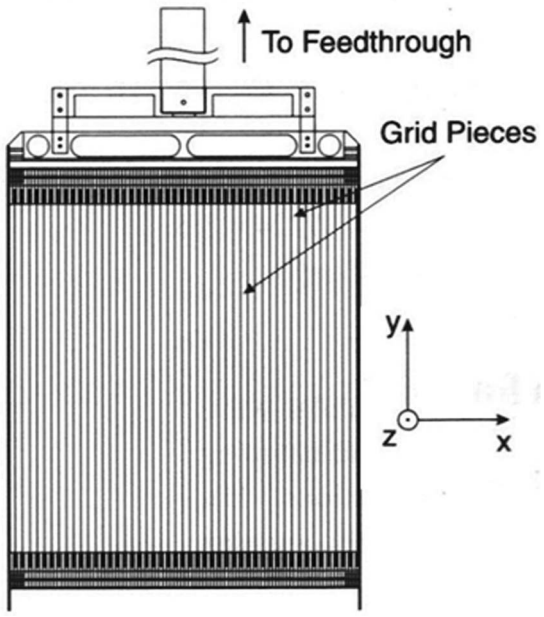

FIG. 3. Diagram of Iowa arbitrary spatial waveform antenna. (Ref. 12).

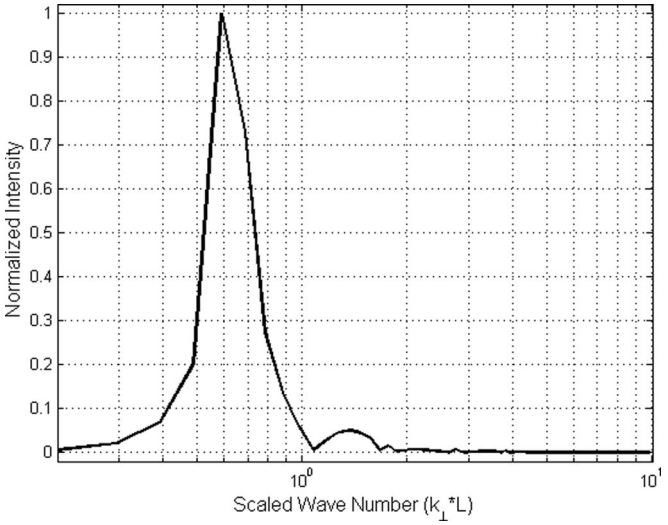

FIG. 4. Calculated k_x spectra based on the tuning pattern for each of the 48 copper mesh elements in the antenna.

allows us to control the frequency response for this circuit at high frequency. Additionally in our experiments, we suppress the drift waves, which typically have frequencies below 100 kHz, by adding an RC circuit on the gain setting impedance of the amplifier.

B. Calibration of probe

We performed an absolute calibration of the magnetic field part of the probe by using a Helmholtz coil in conjunction with an arbitrary waveform generator. The magnetic field is measured at the center of the coils using agaussmeter, and a relationship between coil current and magnetic field is determined at low frequency. The Elsässer probe is then placed at the same position in the coils as the gaussmeter and a relationship between the magnetic field at the input of the probe and the voltage measured at the output of the probe is determined as a function of frequency.

To calibrate the electric field probe a white noise source is used to apply a voltage across the tips of the probe. Cross-correlation of the input and output signals gives the transfer function of the amplifier circuit starting at the probe tips.[26] An additional calibration was performed from the experimental data. Since we have an absolute calibration for the magnetic field data and V_A can be determined from the plasma parameters, the electric field can be calculated from Eq. (8) provided that ω and k_x are known. The result can then be compared with the measured electric field data to determine if the probe is working correctly.

IV. EXPERIMENTAL APPROACH AND ANALYSIS

We briefly describe here the experimental approach for our measurements. Further information can be found in the references for earlier works.[11,12] This experiment was performed in the LaPD at UCLA.[27,28] The LaPD is a 20.7 m long vacuum chamber, which can produce a plasma column of 40–70 cm in diameter. The experiments took place in 50% ionized He plasma[29] 0.1 ms into the afterglow. From a swept Langmuir probe, in conjunction with a microwave interferometer, the density in the measurement region was determined to be 9.0×10^{11} cm^{-3} and the electron temperature was 4.5 eV. The background magnetic field was set to 1850 G, which yields an Alfvén speed of 3.0×10^8 cm/s and puts us in the inertial regime ($V_A > v_{te}$). From these plasma parameters, the electron cyclotron frequency was determined to be 5.1 GHz and the electron skin depth, $\delta_e = c/\omega_{pe}$, was 0.56 cm.

To produce the waves, we are using the Iowa arbitrary spatial waveform antenna described in Ref. 12. This antenna, shown in Fig. 3, consists of a set of 48 vertical copper mesh grids of dimension 2.5 cm × 30.5 cm. Each element is separated by 0.64 cm and can be individually driven by a temporally identical signal with varying amplitudes from 1 to −1. By varying the amplitude of each grid element, we are able to create an arbitrary spatial waveform across the array in the $\hat{x}$ direction with effectively no variation in the $\hat{y}$ direction. This allows us to tune our antenna to produce a planar wave with a specific k_x value.

To tune the antenna effectively to a particular k_x value, we start by tuning each grid element to a value between −1

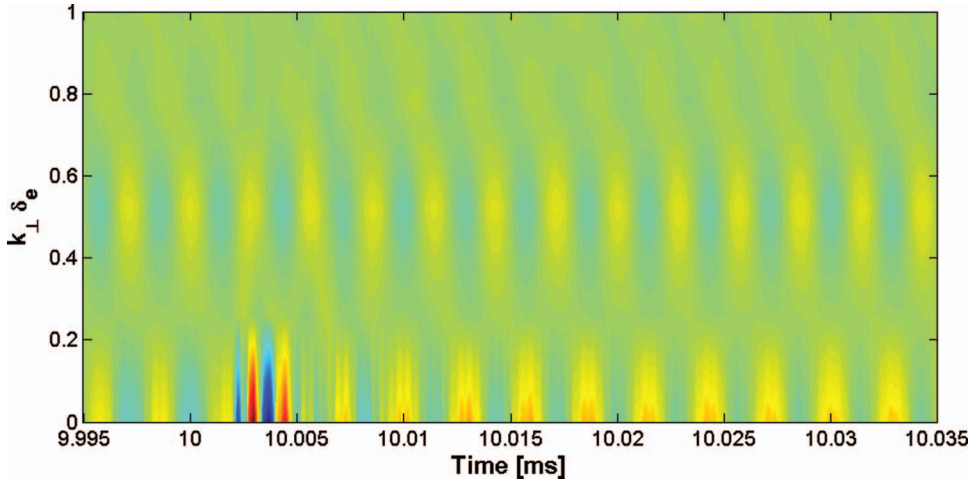

FIG. 5. (Color online) The k_x spectra as a function of time.

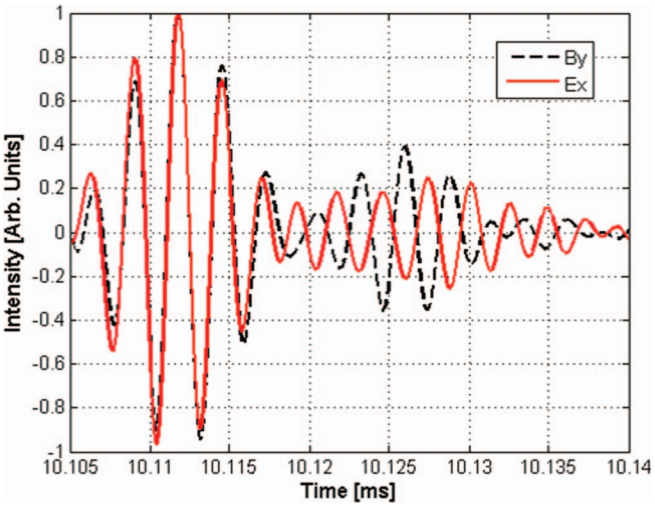

FIG. 6. (Color online) The B_y and E_x components of the $k_x = 0.5$ mode of the Alfvén wave for a short pulse after the plasma is turned off.

and 1. Next, we integrate across all 48 grid elements to determine the approximate configuration of the magnetic field in the $\hat{y}$ direction. A Fourier transform of the magnetic field then provides a good estimate of the k_x spectra for a particular tuning pattern. For the experiments reported here, we have designed a wave with $k_x = 0.6$, see Fig. 4.

A time series was recorded at each spatial position in the plasma with a sampling rate of 12.5 MHz. Since the shot to shot variation in the LaPD is minimal, averaging of 10 shots per spatial position was sufficient to achieve a signal-to-noise ratio of 20. Fourier transforms were performed on the data at every time step to separate each of the k_x components. An example of the k_x spectra as a function of time is shown in Fig. 5. In the figure we can clearly see the shut off of the plasma at t = 10 ms. In addition, two modes are observed at $k_x = 0$ and 0.5. The $k_x = 0$ mode, or coaxial mode, is always present in the plasma at the LaPD since it is very easy to excite. However, this is not an Alfvén wave. For this research we are working with the $k_x = 0.5$ mode, which is an Alfvén wave and was excited by the waveform antenna as seen in Fig. 4.

The B_y and E_x components of the Alfvén wave for this k_x component using a short pulse are shown in Fig. 6. The figure clearly shows two sets of wave packets. The first packet shows B_y and E_x in phase with each other, while the second packet shows that they are out of phase by 180°. Based on the calculated Alfvén speed of 3.0×10^8 cm/s and the distances between the probe and the antenna and the probe and the cathode, we determined that the first wave packet is the incident wave produced by the antenna and the second packet is from reflection off the cathode. By determining the Poynting flux, we can distinguish the incident wave from the reflected wave more effectively. In Fig. 7 we can see the transmitted signal from the antenna (initial peaks) and the reflected signal off the cathode (smaller peaks beginning 0.05 ms later).

In addition to measuring the Poynting flux, we computed the ratio of E_x to B_y from Eq. (9), where $E_x = \Delta V/\Delta x$. We found a value of 3.92×10^9 cm/s, which is much greater than the 3.0×10^8 cm/s calculated from the plasma parameters. However, we have not included the effects of plasma coupling on the electric field. Recall that in Sec. III of the paper we showed that the sheath impedance is 11 times higher than the actual 50 Ω we had in the circuit. Including this factor in the calibration of E_x, we find that the Alfvén speed is 3.57×10^8 cm/s, which is in good agreement with the calculated value from the plasma parameters.

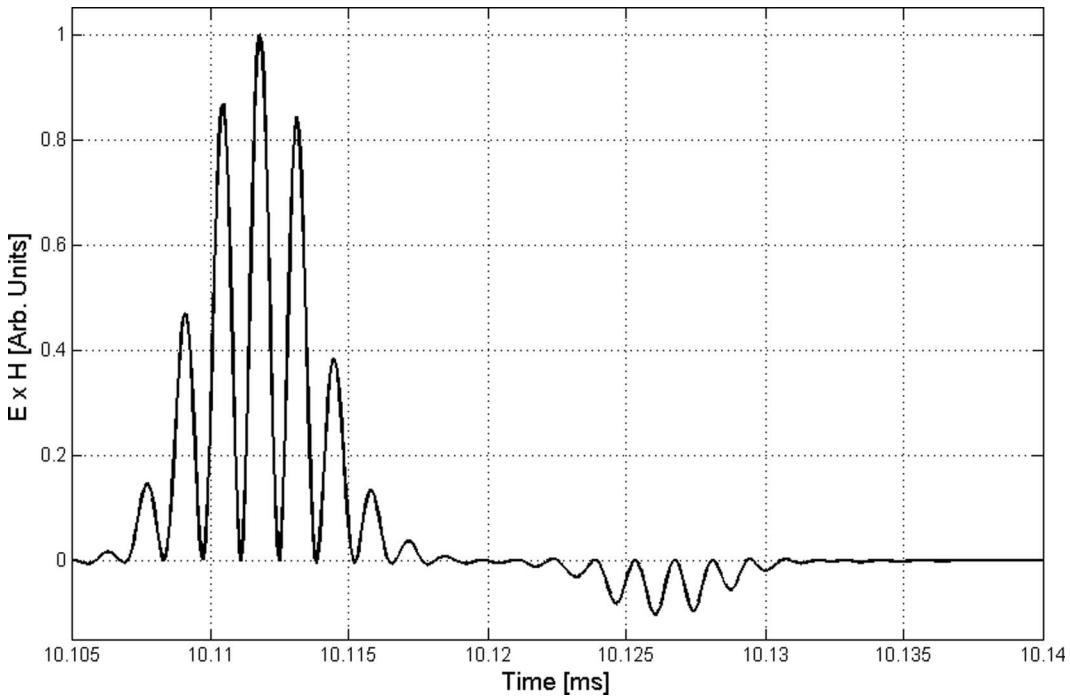

FIG. 7. The Poynting flux as determined from the data in Fig. 6. Shown are the transmitted signal from the antenna (initial peaks) and the reflected signal off the cathode (smaller peaks beginning 0.05 ms later).

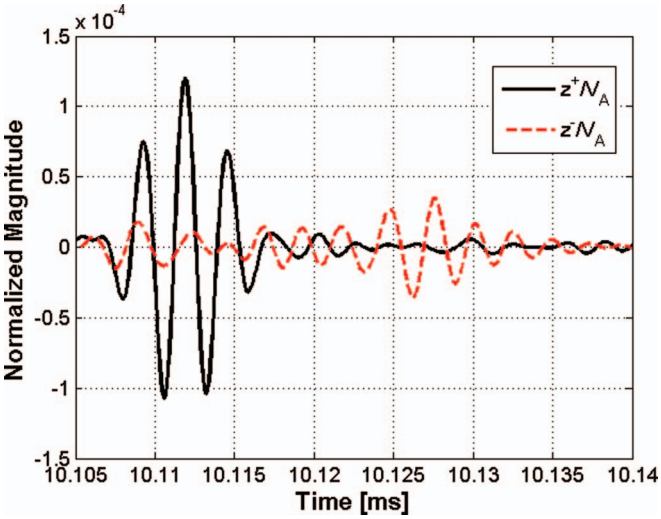

FIG. 8. (Color online) Calculated values of the modified Elsässer variables normalized to V_A.

Another important measurement is that of the error in the intensities of the E_x and B_y spectrum. This error can be estimated from the method of error propagation,

$$\%error = \left\langle \sqrt{\frac{E_x - V_A B_y \sqrt{\left(1 + k_x^2 \delta_e^2\right)\left(1 - \frac{\omega^2}{\Omega^2}\right)}}{|E_x|^2 + \left|V_A B_y \sqrt{\left(1 + k_x^2 \delta_e^2\right)\left(1 - \frac{\omega^2}{\Omega^2}\right)}\right|^2}} \right\rangle. \tag{13}$$

Taking the calculated value of the Alfvén speed and values for the calibrated transmitted peaks of B_y and E_x, where the sheath impedance is included in the calibration, we find that the error in the signal is approximately 20%. Although we did adjust our calculations to take into account that B_y and E_x are measured about 1 cm apart, some of the error in the signal maybe due to the fact that this distance is not exactly 1 cm since the E_x loops were not perfect circles. Another source of systematic error which may account for this difference is that all calibrations were done on a workbench in air and not under laboratory plasma conditions.

Finally, we can use Eq. (5) to determine the generalized Elsässer variables. We present these results in Fig. 8, where we have normalized to V_A. As in the case of Fig. 6, we can easily identify the incident (z^+) and the reflected (z^-) waves using this method. We notice in the figure that part of the z^- wave appears to be present at the beginning of the z^+ wave. This apparent oscillation in the signal is due to the fact that the Alfvén wave pulses emitted by the Iowa spatial waveform antenna have a broad frequency spectrum. In Eq. (5) we calculated the value of $z^\pm$ using only the characteristic frequency of the wave, $f = 350$ kHz. This error could account for part of the 20% error in the Alfvén speed, as determined from Eq. (13).

V. CONCLUSIONS

The prototype Elsässer probe, as described in this paper, was developed to measure electric and magnetic fields in a plasma wave. We tested it using an Alfvén wave propagating in the $\hat{x} - \hat{z}$ plane of the LaPD in 50% ionized He plasma. The results indicate that discreet measurements of the transmitted and reflected signals are readily achievable. Once the sheath impedance was included in the calculations, the error in the signals, as compared to the Alfvén speed, was determined to be about 20%. In addition, we presented calculated values for the modified Elsässer variables normalized to the Alfvén speed. The results show that we are able to measure very small wave fields using this new type of probe.

ACKNOWLEDGMENTS

Funding for this project was provided by National Science Foundation (NSF) (Grant No. ATM 03–17310), Department of Energy (DOE) (Grant No. DE-FG02–06ER54890), and NSF (Grant No. PHY-10033446). The experiments presented here were conducted at the Basic Plasma Science Facility at UCLA, which is funded in part by the U.S. DOE and the NSF.

[1] H. Alfvén, Nature (London) **150**, 405 (1942).
[2] A. Verdini and M. Velli, Astrophys. J. **662**, 669 (2007).
[3] C. C. Chaston, V. Genot, J. W. Bonnell, C. W. Carlson, J. P. McFadden, R. E. Ergun, R. J. Strangeway, E. J. Lund, and K. J. Hwang, J. Geophys. Res. **111**, A03206(14) (2006).
[4] C. A. Kletzing, J. Geophys. Res. **99**, 11095 (1994).
[5] J. R. Wygant, A. Keiling, C. A. Cattell, M. Johnson, R. L. Lysak, M. Temerin, F. S. Mozer, C. A. Kletzing, J. D. Scudder, W. Peterson, C. T. Russell, G. Parks, M. Brittnacher, G. Germany, and J. Span, J. Geophys. Res. **105**, 18675 (2000).
[6] K. L. Wong, R. J. Fonck, S. F. Paul, D. R. Roberts, E. D. Fredrickson, R. Nazikian, H. K. Park, M. Bell, N. L. Bretz, R. Budny, S. Cohen, G. W. Hammett, F. C. Jobes, D. M. Meade, S. S. Medley, D. Mueller, Y. Nagayama, D. K. Owens, and E. J. Synakowski, Phys. Rev. Lett. **66**, 1874 (1991).
[7] M. P. Gryaznevich and S. E. Sharapov, Nucl. Fusion **40**, 907 (2000).
[8] S. V. Mirnov, Atomnaya Énergiya **17**, 209 (1964).
[9] M. A. Van Zeeland, G. J. Kramer, M. E. Austin, R. L. Boivin, W. W. Heidbrink, M. A. Makowski, G. R. McKee, R. Nazikian, W. M. Solomon, and G. Wang, Phys. Rev. Lett. **97**, 135001(4) (2006).
[10] J. Spaleta, L. Zakharov, R. Kaita, R. Majeski, and T. Gray, Rev. Sci. Instrum. **77**, 10E305(3) (2006).
[11] D. J. Thuecks, C. A. Kletzing, F. Skiff, S. R. Bounds, and S. Vincena, Phys. Plasmas **16**, 052110(11) (2009).
[12] C. A. Kletzing, D. J. Thuecks, F. Skiff, S. R. Bounds, and S. Vincena, Phys. Rev. Lett. **104**, 095001(4) (2010).
[13] A. Pederson, F. Mozer, and G. Gustafsson, *Measurement Techniques in Space Plasma Fields*, edited by R. H. Pfaff, J. E. Borovsky, and D. T. Young (American Geophysical Union, Washington, D.C., 1998), pp. 1–12.
[14] P.-A. Lindqvist, G. T. Marklund, and L. G. Blomberg, Space Sci. Rev. **70**, 593 (1994).
[15] A. I. Eriksson, M. André, B. Klecker, H. Laakso, P.-A. Lindqvist, F. Mozer, G. Paschmann, A. Pedersen, J. Quinn, R. Torbert, K. Torkar, and H. Vaith, Ann. Geophys. **24**, 275 (2006).
[16] N. C. Maynard, T. L. Aggson, and J. P. Heppner, J. Geophys. Res. **88**, 3991 (1983).
[17] F. F. Chen, *Modern Uses of Langmuir Probes*, Research Report (Nagoya, Japan, 1985).
[18] W. Horton, Rev. Mod. Phys. **71**, 735 (1999).

[19]V. A. Vershkov, V. V. Dreval, and S. V. Soldatov, Rev. Sci. Instrum. **70**, 1700 (1999).
[20]I. Alexeff and W. D. Jones, Phys. Rev. Lett. **15**, 286 (1965).
[21]A. C. Tribble, J. S Pickett, N. D'Angleo, and G. B. Murphy, Planet. Space Sci. **37**, 1001 (1989).
[22]W. M. Elsässer, Phys. Rev. **79**, 183 (1950).
[23]D. G. Swanson, *Plasma Waves*, 2nd ed. (Institute of Physics, Philadelphia, 2003).
[24]W. Gekelman, S. Vincena, D. Leneman, and J. Maggs, J. Geophys. Res. **102**, 7225 (1997).
[25]L. Schott, *Plasma Diagnostics*, edited by W. Lochte-Holtgreven (American Institute of Physics, New York, 1995), pp. 668–731.
[26]M. Tohyama, H. Suzuki, and Y. Ando, *Nature and Technology of Acoustic Space* (Academic, London, 1995).
[27]D. Leneman, W. Gekelman, and J. Maggs, Rev. Sci. Instrum. **77**, 015108(10) (2006).
[28]W. Gekelman, H. Pfister, Z. Lucky, J. Bamber, D. Leneman, and J. Maggs, Rev. Sci. Instrum. **62**, 2875 (1991).
[29]J. E. Maggs, T. A. Carter, and R. J. Taylor, Phys. Plasmas **14**, 052507 (2007).